nature neuroscience

Unique functional properties of somatostatin-expressing GABAergic neurons in mouse barrel cortex

Luc J Gentet[1,2], Yves Kremer[1], Hiroki Taniguchi[3], Z Josh Huang[3], Jochen F Staiger[4] & Carl C H Petersen[1]

Neocortical GABAergic neurons have diverse molecular, structural and electrophysiological features, but the functional correlates of this diversity are largely unknown. We found unique membrane potential dynamics of somatostatin-expressing (SOM) neurons in layer 2/3 of the primary somatosensory barrel cortex of awake behaving mice. SOM neurons were spontaneously active during periods of quiet wakefulness. However, SOM neurons hyperpolarized and reduced action potential firing in response to both passive and active whisker sensing, in contrast with all other recorded types of nearby neurons, which were excited by sensory input. Optogenetic inhibition of SOM neurons increased burst firing in nearby excitatory neurons. We hypothesize that the spontaneous activity of SOM neurons during quiet wakefulness provides a tonic inhibition to the distal dendrites of excitatory pyramidal neurons. Conversely, the inhibition of SOM cells during active cortical processing likely enhances distal dendritic excitability, which may be important for top-down computations and sensorimotor integration.

Neocortical circuits are primarily driven by excitatory glutamatergic and inhibitory GABAergic synaptic conductances. Although GABAergic neurons account for only ~15% of the total population of neocortical neurons, they exhibit a high degree of molecular, structural and electrophysiological diversity[1–5]. However, the functional correlates of these diverse features have not yet been mapped, presumably because of the technical difficulty of recording from identified GABAergic neurons in awake behaving mammals.

We used two-photon microscopy *in vivo* to target whole-cell membrane potential recordings to genetically defined, GFP-labeled GABAergic neurons in layer 2/3 of the mouse neocortex[6–8]. We focused our investigations on the primary somatosensory barrel cortex, which serves as a useful model system for studying active whisker sensory perception[9–11]. Recently, it was found that most of the GABAergic neurons in layer 2/3 mouse barrel cortex can be assigned to one of three non-overlapping genetically defined classes[12]: parvalbumin-expressing fast-spiking neurons accounting for ~30% of the GABAergic neurons in layer 2/3, 5-HT_{3A}R–expressing and nicotinic acetylcholine receptor–expressing non–fast-spiking (NFS) neurons accounting for ~50% of the GABAergic neurons in layer 2/3, and SOM neurons accounting for ~20% of the GABAergic neurons in layer 2/3. These three molecularly defined classes of GABAergic neurons (fast spiking, NFS and SOM) also have anatomical correlates. Fast-spiking neurons are mainly considered to provide fast GABAergic input at locations electrotonically close to the soma, and they can be divided into two main subtypes, one that innervates soma and proximal dendrites of excitatory neurons[13,14] and one that specifically innervates the axon initial segment[15]. NFS neurons are a more diverse group of GABAergic neurons, but they are known to contain at least two well-defined classes, one type being neurogliaform cells (which may primarily inhibit all surrounding neurons through volume transmission[16]) and the other type being vasoactive intestinal peptide (VIP)-expressing cells (which may preferentially inhibit other nearby GABAergic neurons[17–20]). SOM neurons (which include Martinotti cells) are thought to primarily innervate the distal dendrites of excitatory neurons[21–25] and, according to *in vitro* brain slice experiments, these neurons receive an unusual strongly facilitating excitatory synaptic input from nearby excitatory neurons during high-frequency stimulation[23,24,26,27]. *In vitro* brain slice experiments have shown that both fast-spiking and SOM neurons densely innervate nearby excitatory pyramidal neurons in layer 2/3 mouse cortex[28,29]. The diversity of neocortical GABAergic neurons could imply a specialized function for each subtype in regulating the activity of the local circuit.

Previous recordings from GFP-labeled GABAergic neurons in layer 2/3 barrel cortex of awake mice[7] revealed that fast-spiking cells fire action potentials, on average, at a higher rate than nearby NFS and excitatory neurons. Fast-spiking neurons fire at the highest rates during quiet wakefulness (when the whiskers are not moving), but the spike rate of fast-spiking neurons decreases during active free whisking in air[7]. Although NFS neurons are less active than fast-spiking neurons during quiet wakefulness, these neurons depolarize and increase spike rates during free whisking[7]. The slow large-amplitude membrane potential fluctuations recorded during quiet wakefulness are highly correlated without phase difference in fast-spiking, NFS and excitatory neurons[7]. During active whisking in air, the slow membrane potential fluctuations are suppressed and membrane potential correlations decrease amongst fast-spiking, NFS and excitatory neurons, but remain positive and centered around zero time difference[7].

The activity patterns of neocortical SOM neurons during behavior are currently unknown. We investigated the membrane potential

[1]Laboratory of Sensory Processing, Brain Mind Institute, Faculty of Life Sciences, École Polytechnique Fédérale de Lausanne (EPFL), Switzerland. [2]Swammerdam Institute for Life Sciences, University of Amsterdam, The Netherlands. [3]Cold Spring Harbor Laboratory, Cold Spring Harbor, New York, USA. [4]Department of Neuroanatomy, Georg-August-University, Göttingen, Germany. Correspondence should be addressed to C.C.H.P. (carl.petersen@epfl.ch).

Received 10 November 2011; accepted 17 January 2012; published online 26 February 2012; doi:10.1038/nn.3051

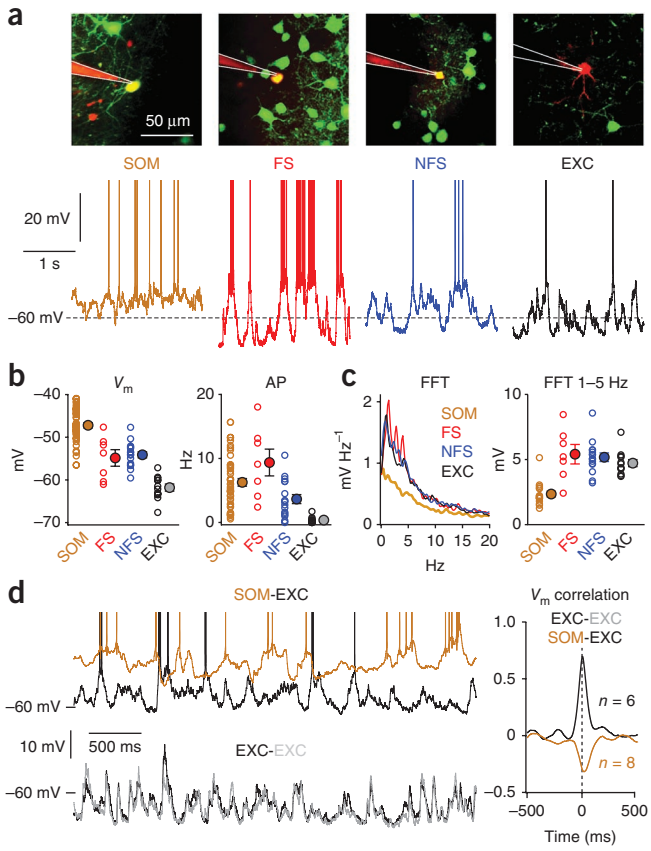

Figure 1 Unique membrane potential dynamics of SOM neurons during quiet wakefulness. (**a**) Example whole-cell recordings of spontaneous membrane potential fluctuations during quiet wakefulness (lower traces) of different classes of genetically identified layer 2/3 neurons visualized by two-photon microscopy (upper images) in head-restrained mice. EXC, excitatory; FS, fast spiking. (**b**) During quiet wakefulness, SOM neurons were depolarized (V_m, left) and fired action potentials (AP) at high rates (right). Each open circle represents an individual neuron and filled circles with error bars represent mean ± s.e.m. (**c**) FFT analysis revealed that SOM neurons had markedly less slow membrane potential fluctuations compared with other layer 2/3 cell types (left), further quantified over the 1–5-Hz frequency range for each recorded neuron (right). Each open circle represents an individual neuron and filled circles with error bars represent mean ± s.e.m. (**d**) Dual whole-cell recordings revealed that membrane potential fluctuations in SOM neurons were weakly anticorrelated with nearby excitatory neurons, whereas membrane potential fluctuations in nearby excitatory neurons were highly correlated.

dynamics of SOM neurons in layer 2/3 of the primary somatosensory barrel cortex of awake head-restrained mice during quantified whisker behavior. We found that SOM neurons have unique membrane potential dynamics that differ in almost every respect from fast-spiking, NFS and excitatory neurons located in the same neocortical microcircuit.

RESULTS

Whole-cell membrane potential recordings were obtained from GFP-labeled neurons in layer 2/3 of the C2 barrel column in *Gad1* (also known as *Gad67*)-*GFP*[30] and *Gin-GFP*[31] mice (**Supplementary Figs. 1** and **2**). Nearly all of the layer 2/3 GABAergic neurons express GFP in *Gad67-GFP* mice[7,30]. As in previous studies[7,8], in our recordings from *Gad67-GFP* mice, we differentiated between fast-spiking and NFS GABAergic neurons. Perhaps because GFP expression levels are low in SOM neurons in *Gad67-GFP* mice[32], we only recorded from one putative SOM neuron in *Gad67-GFP* mice and the data from this cell were not further analyzed (**Supplementary Fig. 3**). In *Gin-GFP* mice, we found that a much smaller number of neurons expressed GFP. Consistent with previous findings[22,31], all GFP-labeled neurons in *Gin-GFP* mice were immunopositive for somatostatin (**Supplementary Figs. 1** and **2**) and we therefore referred to these neurons as SOM neurons. The electrophysiological properties of SOM neurons, including action potential waveform, input resistance and rheobase, differed from fast-spiking and NFS neurons identified in *Gad67-GFP* mice (**Supplementary Fig. 1**). In addition to the three types of GABAergic neurons, we also recorded from excitatory pyramidal neurons that did not express GFP in *Gin-GFP* mice. Thus, we contrasted the membrane potential dynamics of SOM neurons with fast-spiking, NFS and excitatory neurons, all of which were located in layer 2/3 of the C2 barrel column of awake head-restrained mice during quantified whisker behavior filmed with a high-speed (500 Hz) camera.

Membrane potential of SOM neurons during quiet wakefulness

During quiet wakefulness (when the whiskers were not moving), SOM cells were significantly more depolarized than other types of layer 2/3 neurons (SOM, −47.2 ± 0.6 mV, n = 49; fast spiking, −54.8 ± 1.9 mV, n = 7; NFS, −54.1 ± 0.7 mV, n = 18; excitatory, −61.8 ± 0.8 mV, n = 14; P < 0.01 for each cell type compared with SOM) and spontaneously fired action potentials at high rates (SOM, 6.3 ± 0.6 Hz, n = 49; fast spiking, 9.4 ± 2.1 Hz, n = 7; NFS, 3.7 ± 0.7 Hz, n = 18; excitatory, 0.4 ± 0.1 Hz, n = 14; **Fig. 1a**,**b**). Action potential threshold was similar across all classes of layer 2/3 neurons (SOM, −40.3 ± 0.7 mV, n = 44; fast spiking, −40.5 ± 0.7 mV, n = 7; NFS, −41.2 ± 1.1, n = 15; excitatory, −41.0 ± 1.0 mV, n = 10). Although fast-spiking, NFS and excitatory neurons showed prominent slow membrane potential fluctuations during quiet wakefulness[7,33,34], these were not apparent in SOM neurons (**Fig. 1a**). The amplitude of membrane potential fluctuations in the 1–5-Hz frequency range quantified from the integral of the fast Fourier transform (FFT) showed that slow membrane potential oscillations were significantly smaller in SOM neurons than in other types of layer 2/3 neurons (SOM, 2.3 ± 0.2 mV, n = 16; fast spiking, 5.4 ± 0.7 mV, n = 7; NFS, 5.2 ± 0.3 mV, n = 15; excitatory, 4.7 ± 0.3 mV, n = 12; P < 0.01 for each cell type compared with SOM; **Fig. 1c**). Hyperpolarizing SOM cells through current injection did not increase slow membrane potential fluctuations (**Supplementary Fig. 4**).

Dual whole-cell recordings revealed that membrane potential fluctuations in SOM cells were out of phase with those of nearby pyramidal neurons with a peak cross-correlation coefficient of −0.38 ± 0.03 centered at 23 ± 8 ms (n = 8; **Fig. 1d**), with hyperpolarization of SOM neurons occurring significantly later than the depolarization of excitatory neurons (P = 0.03). On the other hand, dual recordings from two excitatory neurons in *Gin-GFP* mice showed highly correlated membrane potential dynamics in phase with each other (peak cross-correlation coefficient of 0.70 ± 0.06 centered at 4 ± 2 ms, n = 6; **Fig. 1d**)[7,33,35]. We previously reported that fast-spiking, NFS and excitatory neurons recorded in *Gad67-GFP* mice have synchronous membrane potential fluctuations during quiet wakefulness[7]. During quiet wakefulness, SOM cells therefore have unique patterns of spontaneous membrane potential fluctuations compared with all other recorded populations of layer 2/3 barrel cortex neurons.

SOM neurons *in vitro* receive excitatory synaptic input with unusual short-term dynamics for the neocortex, with single action potentials only evoking small-amplitude excitatory postsynaptic potentials, which are strongly facilitated during high-frequency action potential

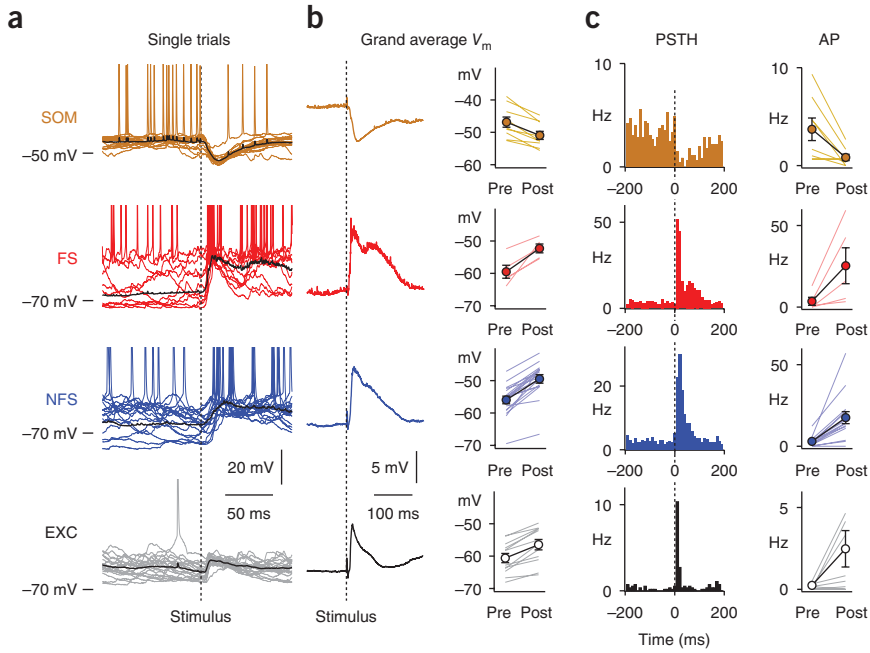

Figure 2 Sensory stimulation hyperpolarizes SOM cells. (**a**) Example whole-cell membrane potential recordings in awake head-restrained mice from different classes of layer 2/3 neurons comparing the sensory responses evoked by brief deflection of the C2 whisker. Single trials are color coded according to cell type. The average response across trials for the given recording is shown superimposed in black. (**b**) The grand average of the sensory-evoked membrane potential response across all recordings from a given class of layer 2/3 neuron (left) and the mean membrane potential in the 50 ms before (pre) compared with the 5–55 ms after stimulus (post) for each individual recording (right). Every SOM neuron hyperpolarized in response to whisker stimulation, whereas every neuron belonging to other classes of layer 2/3 neurons had a depolarizing sensory response. Each thin line represents an individual neuron and filled circles with error bars connected by thick lines represent mean ± s.e.m. (**c**) The grand average peristimulus time histograms across all recordings (left) and the quantification of firing rates (right) in the 50 ms before (pre) compared with the 5–55 ms after stimulation (post) revealed that whisker stimulation reduced action potential firing in SOM neurons, but increased action potential firing in all other classes of layer 2/3 neurons. Each thin line represents an individual neuron and filled circles with error bars connected by thick lines represent mean ± s.e.m.

firing[23,24,26,27]. Similar short-term synaptic dynamics *in vivo* (**Supplementary Fig. 5**) might contribute to the overall weak correlation of spontaneous membrane potential fluctuations in SOM neurons with nearby pyramidal neurons, as high-frequency action potential firing is rare in excitatory layer 2/3 neurons. The delayed hyperpolarization observed in SOM cells might be driven by action potential firing in nearby fast-spiking, NFS or other types of GABAergic neurons.

Whisker sensorimotor input hyperpolarizes SOM cells

We specifically targeted our recordings to the C2 barrel column, which is known to process sensory information relating to the C2 whisker[10]. A single brief C2 whisker deflection evoked a hyperpolarizing sensory response in SOM cells, whereas the sensory response was depolarizing in all other types of recorded layer 2/3 neurons (SOM, −4.1 ± 0.3 mV, n = 10; fast spiking, 7.2 ± 0.6 mV, n = 5; NFS, 6.5 ± 0.1 mV, n = 15; excitatory, 4.1 ± 0.2 mV, n = 11; **Fig. 2a**,**b**). The sensory-evoked hyperpolarization in SOM neurons had a short latency, similar to the latencies for the sensory-evoked depolarization in other types of layer 2/3 neurons (SOM, 9.6 ± 0.9 ms, n = 9; fast spiking, 7.5 ± 1.0 ms, n = 5; NFS, 10.3 ± 0.6 ms, n = 15; excitatory, 10.2 ± 0.4 ms, n = 11). The reversal potential of the sensory-evoked response in SOM cells is consistent with a rapid synaptic activation of ionotropic GABAergic conductances (**Supplementary Fig. 6**). The whisker deflection–evoked hyperpolarization of SOM neurons resulted in a transient reduction in action potential firing, contrasting with the increased action potential firing recorded in layer 2/3 fast-spiking, NFS and excitatory neurons (SOM, −2.9 ± 0.9 Hz, n = 8; fast spiking, 21.8 ± 8.9 Hz, n = 5; NFS, 14.0 ± 3.0 Hz, n = 15; excitatory, 2.2 ± 1.0 Hz, n = 11; **Fig. 2c**). Compared with the other recorded types of neurons in the same neocortical microcircuit, SOM neurons are therefore unique in being inhibited by passive whisker sensory stimulation.

Mice actively acquire sensory information by moving their whiskers back and forth at high frequencies (5–20 Hz)[9–11]. SOM cells rapidly hyperpolarized and reduced action potential firing after the voluntary initiation of free whisking in air (quiet, −45.9 ± 0.9 mV, 6.2 ± 0.7 Hz; whisking, −50.7 ± 0.9 mV, 2.1 ± 0.4 Hz; n = 32, P < 0.001 for both membrane potential and spike rates; **Fig. 3a**,**b** and **Supplementary Fig. 7**). Active whisker-object contacts evoked a small hyperpolarizing sensory response in SOM cells, adding to the already hyperpolarized membrane potential induced by free whisking (**Fig. 3c**,**d**). The inhibition of SOM neurons during active sensing contrasts with the depolarizing responses evoked by active touch in excitatory layer 2/3 neurons[34,36], as well as in both fast-spiking and NFS GABAergic neurons (SOM, −1.0 ± 0.5 mV, n = 6; fast spiking, 2.5 ± 0.1 mV, n = 4; NFS, 2.2 ± 0.8 mV, n = 4). Active touch increased action potential firing rates in fast-spiking and NFS neurons[34], but not in SOM cells (SOM, before = 1.5 ± 0.7 Hz, after = 1.7 ± 0.9 Hz, n = 9; fast spiking, before = 7.9 ± 2.4 Hz, after = 12.5 ± 4.4 Hz, n = 4; NFS, before = 3.0 ± 1.6 Hz, after = 7.0 ± 2.3 Hz, n = 4). SOM neurons therefore form the only class of neurons recorded in layer 2/3 barrel cortex that were not excited by active touch.

Inhibition of SOM neurons enhances dendritic excitability

SOM neurons prominently innervate layer 1 of the neocortex[21–25]. The high spontaneous firing rate of SOM cells during quiet wakefulness might therefore tonically inhibit the distal layer 1 dendrites of excitatory cortical pyramidal neurons. The reduced firing of SOM neurons during whisker-related sensorimotor processing might release the inhibitory clamp of distal layer 1 dendrites. Reduced distal dendritic inhibition during active sensing could enable layer 1 input to drive dendritic sodium, calcium and NMDA spikes, enhancing action potential burst firing in excitatory pyramidal neurons[37–40]. Consistent with such a hypothesis, we found a marked increase in layer 1 dendritic calcium signals during whisking (**Fig. 3e**,**f** and **Supplementary Movie 1**), as measured by expression of the genetically encoded calcium indicator GCaMP3 (ref. 41). Reduced action potential firing in SOM neurons therefore correlates with enhanced dendritic calcium signaling during whisking, but it is important to note that other behavior-correlated changes in neural circuits and neuromodulators might also contribute.

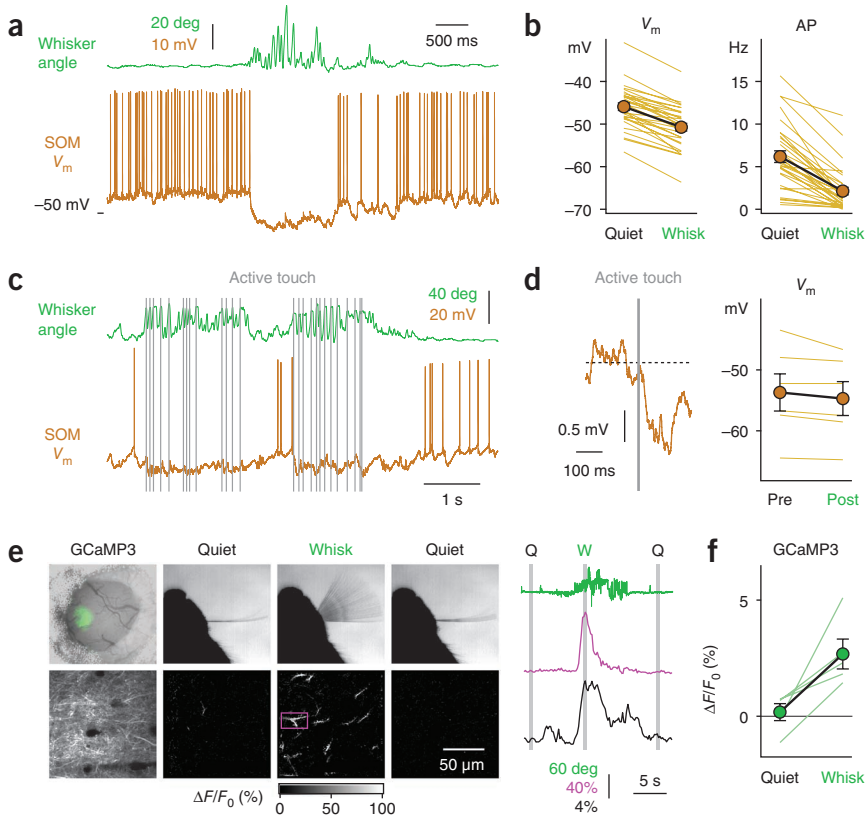

Figure 3 SOM cells hyperpolarize during active whisking and active touch. (**a**) An example whole-cell membrane potential recording from a SOM neuron during free whisking, in the absence of whisker-object contacts (green trace, quantification of whisker angle). (**b**) SOM neurons robustly hyperpolarized and reduced action potential firing during free whisking periods compared to quiet periods. Each thin line represents an individual neuron and filled circles with error bars connected by thick lines represent mean ± s.e.m. (**c**) An example recording from a SOM neuron during active touch, when the mouse voluntarily moves its whisker back and forth, repetitively touching an object (vertical gray lines indicate whisker-object contacts). (**d**) The grand average active touch membrane potential response aligned to the time of whisker-object contact for all recorded SOM neurons. Active touch evoked a small additional hyperpolarization on top of the already hyperpolarized membrane potential induced by whisking. Each thin line represents an individual neuron and filled circles with error bars connected by a thick line represent mean ± s.e.m. (**e**) GCaMP3 fluorescence was imaged through a cranial window (wide field epifluorescence image, field of view = 2.7 mm, upper left; two-photon image of L1 dendrites, lower left). During whisking (top, behavioral images are minimal projections over a 1-s period), large increases in fluorescence were readily observed in L1 dendrites. Whisker angle (green trace, right) was plotted (gray shading highlights the three periods shown in the images on the left; Q, quiet; W, whisking) with quantification of single dendrite fluorescence (purple trace, dendrite highlighted in image by purple box) and whole-field dendritic fluorescence (black trace). (**f**) Whisking induced a robust increase in dendritic GCaMP3 fluorescence. Each thin line corresponds to measurements from an individual mouse and indicates the average change in fluorescence across dendrites in the field of view averaged across multiple whisking episodes. Filled circles with error bars connected by a thick line represent mean ± s.e.m.

To obtain causal evidence for a functional role of SOM neurons, we specifically expressed the light-activated chloride pump halorhodopsin (eNpHR3.0)[42] in SOM neurons expressing Cre recombinase (**Supplementary Figs. 8** and **9**)[43]. Yellow light rapidly and efficiently hyperpolarized SOM neurons expressing halorhodopsin (–27.3 ± 3.6 mV, $n = 4$) and completely abolished action potential firing (light off = 6.8 ± 1.7 Hz, light on = 0.0 ± 0.0 Hz, $n = 7$; **Fig. 4a**,**b**). Optogenetic inhibition of SOM neurons did not affect the slow membrane potential dynamics recorded in nearby excitatory neurons during quiet wakefulness (**Fig. 4c**,**d**). However, optogenetic inhibition of SOM neurons increased action potential firing rate by 83% in nearby excitatory neurons (light off = 1.2 ± 0.2 Hz, light on = 2.2 ± 0.3 Hz, $n = 10$, $P < 0.05$) and strongly enhanced action potential burst firing by 222% (light off = 0.09 ± 0.02 Hz, light on = 0.29 ± 0.09 Hz, $n = 10$, $P < 0.05$; **Fig. 4c**,**e**). The spontaneous high firing rates of SOM cells during quiet wakefulness therefore inhibit excitatory neurons and prevent burst firing.

DISCUSSION

Our measurements in layer 2/3 of the C2 barrel column of awake head-restrained mice reveal that the membrane potential dynamics of SOM neurons are very different from those of fast-spiking, NFS and excitatory neurons. During quiet wakefulness, SOM neuron membrane potential was weakly anticorrelated with the network of highly correlated fast-spiking, NFS and excitatory neurons (**Fig. 1d**)[7]. During passive whisker deflection (**Fig. 2**) or active touch involving whisker palpation of an object (**Fig. 3**), SOM neurons hyperpolarized, whereas fast-spiking, NFS and excitatory neurons depolarized. There are two obvious possibilities to account for these unique membrane potential dynamics of SOM cells in awake behaving mice. First, SOM neurons might lack an important excitatory input that is common to layer 2/3 fast-spiking, NFS and excitatory neurons. Second, SOM neurons might receive more (or a unique type of) inhibitory input relative to layer 2/3 fast-spiking, NFS and excitatory neurons. Action potential firing rates in layer 2/3 excitatory neurons are low (median ~0.1 Hz) and the majority of action potentials in layer 2/3 excitatory neurons occur as single isolated action potentials. Under these conditions, the excitatory synapses from most layer 2/3 excitatory neurons onto postsynaptic SOM neurons likely transmit little depolarization, as high-frequency firing of excitatory neurons appears to be necessary to evoke large amplitude unitary excitatory postsynaptic potentials (**Supplementary Fig. 5**)[23,24,26,27]. In contrast, synaptic transmission from excitatory neurons onto synaptically connected postsynaptic fast-spiking, NFS or excitatory neurons usually show reliable unitary excitatory postsynaptic potentials in response to single action potentials[23,24,26]. In this dynamic view of synaptic connectivity, SOM neurons appear to lack an important component of the excitatory synaptic input compared with fast-spiking, NFS or excitatory neurons, and this might contribute to the absence of a depolarizing sensory response in SOM neurons. In addition, there is also evidence supporting strong inhibitory input onto SOM neurons from other nearby classes of GABAergic neurons. Layer 2/3 SOM neurons in mouse somatosensory cortex receive inhibitory input from all cortical layers, with the strongest inhibition originating

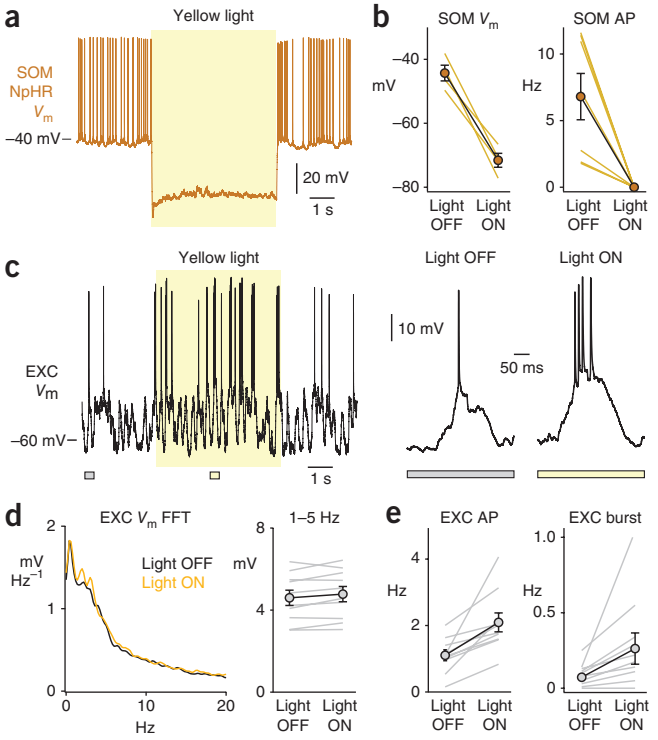

Figure 4 Optogenetic inhibition of SOM neurons increases action potential firing and burst firing in nearby excitatory neurons. (**a**) Example whole-cell recording from a somatostatin (*Sst*)-*cre* neuron expressing halorhodopsin (eNpHR3.0). The yellow light pulse (5-s duration) is indicated by the yellow shading. (**b**) Yellow light evoked robust hyperpolarization and completely blocked action potential firing in *Sst-cre* neurons expressing halorhodopsin. Each thin line represents an individual neuron and filled circles with error bars connected by thick lines represent mean ± s.e.m. (**c**) Example whole-cell recording from an excitatory neuron during optogenetic inhibition of nearby SOM neurons. (**d**) Optogenetic inhibition of SOM neurons did not alter the slow membrane potential dynamics in nearby excitatory neurons during quiet wakefulness. Each thin line represents an individual neuron and filled circles with error bars connected by a thick line represents mean ± s.e.m. (**e**) Optogenetic inhibition of SOM neurons increased action potential firing and burst firing in nearby excitatory neurons. Each thin line represents an individual neuron and filled circles with error bars connected by thick lines represent mean ± s.e.m.

from layers 2, 3 and 4 (ref. 44). Furthermore, anatomical studies provide evidence that VIP-expressing GABAergic neurons might strongly inhibit SOM neurons[1,18,19]. Future experiments involving further quantitative cell type–specific and layer-specific analyses of microcircuit synaptic connectivity and functional operation during behavior are clearly essential to gain a more detailed mechanistic understanding of the origins of the synaptic conductances inhibiting SOM neurons.

An important finding from our recordings in layer 2/3 barrel cortex of awake mice is that SOM neurons were tonically active during quiet wakefulness, but they decreased their action potential output during passive and active whisker sensorimotor processing. SOM neurons densely innervate nearby excitatory neurons in mouse layer 2/3 cortex[28]. SOM neurons send dense axonal arborizations into layer 1 of the neocortex, an unusual cortical layer with few neuronal somata but many dendrites and synapses. During quiet wakefulness, the distal layer 1 dendrites of excitatory pyramidal neurons may therefore be tonically inhibited by the spontaneous action potential firing of SOM neurons. However, during active cortical processing, SOM neurons turn off, likely relieving the distal layer 1 dendrites of excitatory pyramidal neurons from inhibition. With reduced inhibition, the excitatory synaptic inputs onto the distal layer 1 dendrites of excitatory pyramidal neurons are likely to have an enhanced importance. *In vitro* measurements indicate that excitatory glutamatergic inputs onto the distal dendrites of pyramidal neurons can drive somatic burst firing and regenerative dendritic events, such as sodium, calcium and NMDA spikes[37–40]. Notably, *in vitro* measurements have also shown that GABAergic inhibition can regulate the generation of such dendritic events[37]. Our *in vivo* findings of increased layer 1 dendritic calcium levels during whisking (**Fig. 3e**,**f**) and strongly enhanced burst firing during optogenetic inhibition of SOM neurons (**Fig. 4c**,**e**) are consistent with the idea that SOM neurons have a prominent role in the regulation of distal dendritic excitability. Layer 1 of the mouse barrel cortex contains a high density of axon originating from excitatory neurons in primary whisker motor cortex[45]. Decreased action potential firing in SOM neurons during active sensorimotor processing is therefore predicted to enhance the effect of motor cortex input onto excitatory neurons in primary somatosensory cortex potentially driving burst firing and regenerative dendritic events. Such enhanced motor input to sensory cortex gated by SOM neurons might be important for sensorimotor integration, an essential step in active whisker perception[9–11,36,46]. In addition to motor cortex, there are many other brain areas that send axonal fibers to layer 1, and SOM neurons could be important in the regulation of their effect on distal dendritic excitability. In general, across different cortical areas examined, layer 1 axons originate in part from higher order areas, which could mediate top-down control of sensory processing[47]. We speculate that SOM cells will hyperpolarize and reduce action potential firing whenever a given cortical area is actively involved in processing behaviorally relevant information. Decreased firing of SOM cells might reduce GABAergic inhibition onto distal dendrites, thereby enhancing the integration of top-down layer 1 inputs and providing a potentially important mechanism for gating context-dependent processing and binding of different streams of information in the neocortex.

METHODS

Methods and any associated references are available in the online version of the paper at http://www.nature.com/natureneuroscience/.

Note: Supplementary information is available on the Nature Neuroscience website.

ACKNOWLEDGMENTS

We thank L. Looger (Howard Hughes Medical Institute, Janelia Farm) for GCaMP3 and K. Deisseroth (Stanford University) for eNpHR3.0. This work was funded by grants from the Swiss National Science Foundation (C.C.H.P.), Human Frontiers in Science Program (C.C.H.P.), SystemsX.ch (C.C.H.P.) and Deutsche Forschungsgemeinschaft (Sta 431/8-1, 10-1 to J.F.S.), and a joint Deutsche Forschungsgemeinschaft/Swiss National Science Foundation grant Bacofun (C.C.H.P. and J.F.S.).

AUTHOR CONTRIBUTIONS

L.J.G. carried out all of the membrane potential recordings and analyzed the data. Y.K. carried out all of the GCaMP3 imaging experiments and analyzed the data. H.T. and Z.J.H. provided unpublished genetically engineered mice. J.F.S. carried out all of the immunohistochemistry and analyzed the data. C.C.H.P. contributed to the design of experiments, supervised the project and wrote the manuscript. All of the authors commented on the manuscript.

COMPETING FINANCIAL INTERESTS

The authors declare no competing financial interests.

Published online at http://www.nature.com/natureneuroscience/.
Reprints and permissions information is available online at http://www.nature.com/reprints/index.html.

1. Freund, T.F. & Buzsáki, G. Interneurons of the hippocampus. *Hippocampus* **6**, 347–470 (1996).
2. Markram, H. *et al.* Interneurons of the neocortical inhibitory system. *Nat. Rev. Neurosci.* **5**, 793–807 (2004).
3. Ascoli, G.A. *et al.* Petilla terminology: nomenclature of features of GABAergic interneurons of the cerebral cortex. *Nat. Rev. Neurosci.* **9**, 557–568 (2008).
4. Burkhalter, A. Many specialists for suppressing cortical excitation. *Front. Neurosci.* **2**, 155–167 (2008).
5. Klausberger, T. & Somogyi, P. Neuronal diversity and temporal dynamics: the unity of hippocampal circuit operations. *Science* **321**, 53–57 (2008).
6. Margrie, T.W. *et al.* Targeted whole-cell recordings in the mammalian brain *in vivo*. *Neuron* **39**, 911–918 (2003).
7. Gentet, L.J., Avermann, M., Matyas, F., Staiger, J.F. & Petersen, C.C.H. Membrane potential dynamics of GABAergic neurons in the barrel cortex of behaving mice. *Neuron* **65**, 422–435 (2010).
8. Mateo, C. *et al. In vivo* optogenetic stimulation of neocortical excitatory neurons drives brain-state-dependent inhibition. *Curr. Biol.* **21**, 1593–1602 (2011).
9. Brecht, M. Barrel cortex and whisker-mediated behaviors. *Curr. Opin. Neurobiol.* **17**, 408–416 (2007).
10. Petersen, C.C.H. The functional organization of the barrel cortex. *Neuron* **56**, 339–355 (2007).
11. Diamond, M.E., von Heimendahl, M., Knutsen, P.M., Kleinfeld, D. & Ahissar, E. 'Where' and 'what' in the whisker sensorimotor system. *Nat. Rev. Neurosci.* **9**, 601–612 (2008).
12. Lee, S., Hjerling-Leffler, J., Zagha, E., Fishell, G. & Rudy, B. The largest group of superficial neocortical GABAergic interneurons expresses ionotropic serotonin receptors. *J. Neurosci.* **30**, 16796–16808 (2010).
13. Bartos, M., Vida, I. & Jonas, P. Synaptic mechanisms of synchronized gamma oscillations in inhibitory interneuron networks. *Nat. Rev. Neurosci.* **8**, 45–56 (2007).
14. Freund, T.F. & Katona, I. Perisomatic inhibition. *Neuron* **56**, 33–42 (2007).
15. Somogyi, P. A specific 'axo-axonal' interneuron in the visual cortex of the rat. *Brain Res.* **136**, 345–350 (1977).
16. Oláh, S. *et al.* Regulation of cortical microcircuits by unitary GABA-mediated volume transmission. *Nature* **461**, 1278–1281 (2009).
17. Acsády, L., Görcs, T.J. & Freund, T.F. Different populations of vasoactive intestinal polypeptide-immunoreactive interneurons are specialized to control pyramidal cells or interneurons in the hippocampus. *Neuroscience* **73**, 317–334 (1996).
18. Dalezios, Y., Luján, R., Shigemoto, R., Roberts, J.D. & Somogyi, P. Enrichment of mGluR7a in the presynaptic active zones of GABAergic and non-GABAergic terminals on interneurons in the rat somatosensory cortex. *Cereb. Cortex* **12**, 961–974 (2002).
19. Staiger, J.F., Masanneck, C., Schleicher, A. & Zuschratter, W. Calbindin-containing interneurons are a target for VIP-immunoreactive synapses in rat primary somatosensory cortex. *J. Comp. Neurol.* **468**, 179–189 (2004).
20. Dávid, C., Schleicher, A., Zuschratter, W. & Staiger, J.F. The innervation of parvalbumin-containing interneurons by VIP-immunopositive interneurons in the primary somatosensory cortex of the adult rat. *Eur. J. Neurosci.* **25**, 2329–2340 (2007).
21. Wang, Y. *et al.* Anatomical, physiological and molecular properties of Martinotti cells in the somatosensory cortex of the juvenile rat. *J. Physiol. (Lond.)* **561**, 65–90 (2004).
22. Ma, Y., Hu, H., Berrebi, A.S., Mathers, P.H. & Agmon, A. Distinct subtypes of somatostatin-containing neocortical interneurons revealed in transgenic mice. *J. Neurosci.* **26**, 5069–5082 (2006).
23. Kapfer, C., Glickfeld, L.L., Atallah, B.V. & Scanziani, M. Supralinear increase of recurrent inhibition during sparse activity in the somatosensory cortex. *Nat. Neurosci.* **10**, 743–753 (2007).
24. Silberberg, G. & Markram, H. Disynaptic inhibition between neocortical pyramidal cells mediated by Martinotti cells. *Neuron* **53**, 735–746 (2007).
25. McGarry, L.M. *et al.* Quantitative classification of somatostatin-positive neocortical interneurons identifies three interneuron subtypes. *Front. Neural Circuits* **4**, 12 (2010).
26. Reyes, A. *et al.* Target cell–specific facilitation and depression in neocortical circuits. *Nat. Neurosci.* **1**, 279–285 (1998).
27. Fanselow, E.E., Richardson, K.A. & Connors, B.W. Selective, state-dependent activation of somatostatin-expressing inhibitory interneurons in mouse neocortex. *J. Neurophysiol.* **100**, 2640–2652 (2008).
28. Fino, E. & Yuste, R. Dense inhibitory connectivity in neocortex. *Neuron* **69**, 1188–1203 (2011).
29. Packer, A.M. & Yuste, R. Dense, unspecific connectivity of neocortical parvalbumin-positive interneurons: a canonical microcircuit for inhibition? *J. Neurosci.* **31**, 13260–13271 (2011).
30. Tamamaki, N. *et al.* Green fluorescent protein expression and colocalization with calretinin, parvalbumin, and somatostatin in the GAD67-GFP knock-in mouse. *J. Comp. Neurol.* **467**, 60–79 (2003).
31. Oliva, A.A., Jiang, M., Lam, T., Smith, K.L. & Swann, J.W. Novel hippocampal interneuronal subtypes identified using transgenic mice that express green fluorescent protein in GABAergic interneurons. *J. Neurosci.* **20**, 3354–3368 (2000).
32. Suzuki, N. & Bekkers, J.M. Inhibitory neurons in the anterior piriform cortex of the mouse: classification using molecular markers. *J. Comp. Neurol.* **518**, 1670–1687 (2010).
33. Poulet, J.F.A. & Petersen, C.C.H. Internal brain state regulates membrane potential synchrony in barrel cortex of behaving mice. *Nature* **454**, 881–885 (2008).
34. Crochet, S., Poulet, J.F.A., Kremer, Y. & Petersen, C.C.H. Synaptic mechanisms underlying sparse coding of active touch. *Neuron* **69**, 1160–1175 (2011).
35. Okun, M. & Lampl, I. Instantaneous correlation of excitation and inhibition during ongoing and sensory-evoked activities. *Nat. Neurosci.* **11**, 535–537 (2008).
36. O'Connor, D.H., Peron, S.P., Huber, D. & Svoboda, K. Neural activity in barrel cortex underlying vibrissa-based object localization in mice. *Neuron* **67**, 1048–1061 (2010).
37. Larkum, M.E., Zhu, J.J. & Sakmann, B. A new cellular mechanism for coupling inputs arriving at different cortical layers. *Nature* **398**, 338–341 (1999).
38. Losonczy, A., Makara, J.K. & Magee, J.C. Compartmentalized dendritic plasticity and input feature storage in neurons. *Nature* **452**, 436–441 (2008).
39. Larkum, M.E., Nevian, T., Sandler, M., Polsky, A. & Schiller, J. Synaptic integration in tuft dendrites of layer 5 pyramidal neurons: a new unifying principle. *Science* **325**, 756–760 (2009).
40. Branco, T. & Häusser, M. Synaptic integration gradients in single cortical pyramidal cell dendrites. *Neuron* **69**, 885–892 (2011).
41. Tian, L. *et al.* Imaging neural activity in worms, flies and mice with improved GCaMP calcium indicators. *Nat. Methods* **6**, 875–881 (2009).
42. Gradinaru, V. *et al.* Molecular and cellular approaches for diversifying and extending optogenetics. *Cell* **141**, 154–165 (2010).
43. Taniguchi, H. *et al.* A resource of Cre driver lines for genetic targeting of GABAergic neurons in cerebral cortex. *Neuron* **71**, 995–1013 (2011).
44. Xu, X. & Callaway, E.M. Laminar specificity of functional input to distinct types of inhibitory cortical neurons. *J. Neurosci.* **29**, 70–85 (2009).
45. Petreanu, L., Mao, T., Sternson, S.M. & Svoboda, K. The subcellular organization of neocortical excitatory connections. *Nature* **457**, 1142–1145 (2009).
46. Curtis, J.C. & Kleinfeld, D. Phase-to-rate transformations encode touch in cortical neurons of a scanning sensorimotor system. *Nat. Neurosci.* **12**, 492–501 (2009).
47. Gilbert, C.D. & Sigman, M. Brain states: top-down influences in sensory processing. *Neuron* **54**, 677–696 (2007).

ONLINE METHODS

All experimental procedures were approved by the Swiss Federal Veterinary Office.

Whole-cell recordings in awake head-restrained mice. *Gin-GFP*[31], *Gad67-GFP*[30] and somatostatin (*Sst*)-*cre*[43] mice were implanted with metal head-fixation posts, trained for head-restraint, and subsequently electrophysiological recordings were targeted to the C2 barrel column identified through intrinsic signal optical imaging[7,33,34]. All whiskers except C2 were trimmed before the recording session. Passive whisker stimuli were delivered by attaching the C2 whisker to a piezo-bender and delivering 2-ms deflections with maximal angular displacement of ~1 degree. Whisker movements and whisker-object contacts were filmed at 500 Hz and quantified off-line. Whole-cell recordings were targeted to neuronal somata under visual control through two-photon microscopy[6–8]. The pipette solution (adjusted to pH 7.3 with KOH) contained 135 mM potassium gluconate, 4 mM KCl, 10 mM HEPES, 10 mM sodium phosphocreatine, 4 mM MgATP, 0.3 mM Na_3GTP, 0.01 mM Alexa 594 and 2 mg ml^{-1} biocytin (for *post hoc* anatomical identification).

The membrane potential was not corrected for liquid junction potential. Action potential half-width and threshold, and input resistance were measured as previously described[7]. Maximal firing rates were measured from the maximal current pulse injected into each cell and are likely to be underestimates. Rheobase was estimated by determining the lowest current pulse amplitude (increasing in steps of 50 pA) needed to elicit an action potential. FFTs were computed as magnitudes in IgorPro for 5-s segments of the recordings. The low-frequency (1–5 Hz) power was calculated by integrating the computed FFTs from 1 to 5 Hz. Cross-correlations of membrane potential changes were computed by subtracting the average value of each trace, normalizing each trace to its s.d. and then computing the correlation in IgorPro to generate a cross-correlogram with a maximal value of 1 for identical traces[7,33,34]. Analysis of cross-correlation peak time was performed by fitting a Gaussian function around the peak from −80 ms to +80 ms. We took the absolute (positive) time of the cross-correlation peak for excitatory versus excitatory neurons. Membrane potential and firing rate changes in response to passive whisker deflection or active touch were computed over a period of 50 ms preceding the sensory event (denoted by pre) and a period of 50 ms starting 5 ms following the sensory event (denoted by post). All values are mean ± s.e.m. Statistical testing using Student's *t* test was performed in Microsoft Excel.

Functional imaging of GCaMP3 fluorescence in layer 1 dendrites. Adeno-associated virus encoding GCaMP3 (AAV2/1.hSynap.GCaMP3.3.SV40 for C57BL6J mice or AAV2/1.hSynap.Flex.GCaMP3.3.SV40 for *Emx1-cre* mice; Penn Vector Core, University of Pennsylvania)[41] was injected (25–150 nl) into layer 2/3 (250–300 µm below the pia) of the mouse C2 barrel column (identified through intrinsic signal optical imaging) and a cranial window was then implanted[48]. Images were acquired at 5–10 Hz using a modified MOM two-photon microscope (Sutter Instruments) controlled through Labview with Helioscan software[49]. Images were registered using TurboReg[50] and further analyzed using custom routines in ImageJ and Matlab. Applying a threshold to the maximum projection for each movie defined the mask for the region of interest. Quiet and whisking periods were identified based on the high-speed whisker filming. Changes in fluorescence relative to baseline were quantified as mean ± s.e.m.; statistical testing using Student's paired *t* test was performed in Microsoft Excel.

Optogenetic inhibition of SOM cells. Mice expressing Cre recombinase specifically in SOM neurons[43] were injected with AAV-DIO-eNpHR3.0-YFP[42]. Approximately 500 nl of virus with a titer of 1.2×10^{13} genome copies per ml (virus was made and titered by Penn Vector Core, University of Pennsylvania) were injected at a depth of 200–300 µm below the pial surface into the C2 barrel column localized through intrinsic signal optical imaging. Yellow light from an LED (7 mW) was delivered through the 40× objective of the two-photon microscope. Repeated 5-s pulses of yellow light applied every 10 s evoked highly reproducible hyperpolarizations of SOM neurons without noticeable rundown of the optogenetic inhibition over ten repetitions. To study the effects of optogenetic inhibition of SOM cells on the action potential firing of surrounding excitatory neurons, we injected a small amount of depolarizing current (50–200 pA) into the excitatory neuron in most recordings (9 of 10) to obtain a spontaneous firing rate during quiet wakefulness of around 1 Hz. Action potential burst firing was defined as two or more action potentials occurring with interspike intervals of less than 25 ms.

***Gin-GFP* and *Gad67-GFP* cell counts.** Three-dimensional confocal images were obtained from primary somatosensory barrel cortex of fixed 100-µm-thick slices from three *Gad67-GFP* mice and three *Gin-GFP* mice co-stained with DAPI. Cells were manually counted in a layer 2/3 volume of 300 × 300 × 100 µm for *Gad67-GFP* mice and 600 × 300 × 100 µm for *Gin-GFP* mice. Cell counts were scaled to give the number of cells in a volume of 300 × 300 × 300 µm, which is close to the volume of layer 2/3 in the mouse C2 barrel column (see **Supplementary Fig. 1a**).

GFP and somatostatin immunohistochemistry. Coronal sections (50 µm) from the fixed brains were stained for GFP and somatostatin following previously described procedures[7,20]. After rinsing in Tris-buffered saline (TBS, 0.05 M, pH 7.6), the slices were incubated with primary antisera (goat antibody to GFP from Abcam, diluted 1:2,000; rabbit antibody to somatostatin-14 from Bachem, diluted 1:5,000) in TBS containing 0.5% Triton X-100 (TBST, vol/vol) for ~60 h at 6 °C. After rinsing, secondary antisera (Alexa 488–coupled donkey antibody to goat and Alexa 594–coupled donkey antibody to rabbit, both from Invitrogen and diluted 1:500 in TBST) were applied for 4 h at 20–25 °C. After further rinsing, DAPI staining (1:1,000 in TBS for 10 min) was carried out to visualize barrels and layer boundaries. The sections were imaged with a structured illumination microscope (Zeiss AxioImager with Apotome). Cell counts and colocalization were manually scored using Neurolucida (MicroBrightField) (see **Supplementary Figs. 1b**, **2** and **8**).

48. Holtmaat, A. *et al.* Long-term, high-resolution imaging in the mouse neocortex through a chronic cranial window. *Nat. Protoc.* **4**, 1128–1144 (2009).
49. Langer, D., van t'Hoff, M. & Helmchen, F. Helioscan, a highly versatile control software for laser-scanning microscopes written in LabVIEW. Brain Research Institute, University of Zurich, Switzerland (http://www.helioscan.org/) (2010).
50. Thévenaz, P., Ruttimann, U.E. & Unser, M. A pyramid approach to subpixel registration based on intensity. *IEEE Trans. Image Process.* **7**, 27–41 (1998).

Supplementary Information

Unique functional properties of somatostatin-expressing GABAergic neurons in mouse barrel cortex

Luc Gentet, Yves Kremer, Hiroki Taniguchi,
Josh Huang, Jochen Staiger and Carl Petersen

Contents of the Supplementary Information:

1. Supplementary Figure 1 – Properties of GIN-GFP & GAD67-GFP cells
2. Supplementary Figure 2 – GIN-GFP vs SOM immunohistochemistry
3. Supplementary Figure 3 – SOM-like cell in GAD67-GFP mouse
4. Supplementary Figure 4 – Vm dynamics during quiet wakefulness
5. Supplementary Figure 5 – Vm correlations in a connected pair
6. Supplementary Figure 6 – Reversal potential of sensory response
7. Supplementary Figure 7 – Rapid hyperpolarization after whisking onset
8. Supplementary Figure 8 – Expression of NpHR3-YFP in SOM-Cre cells
9. Supplementary Figure 9 – SOM-Cre cells similar to SOM-GIN-GFP cells
10. Supplementary Movie 1 – GCaMP3 imaging of layer 1 dendrites

Nature Neuroscience: doi:10.1038/nn.3051

Supplementary Figure 1

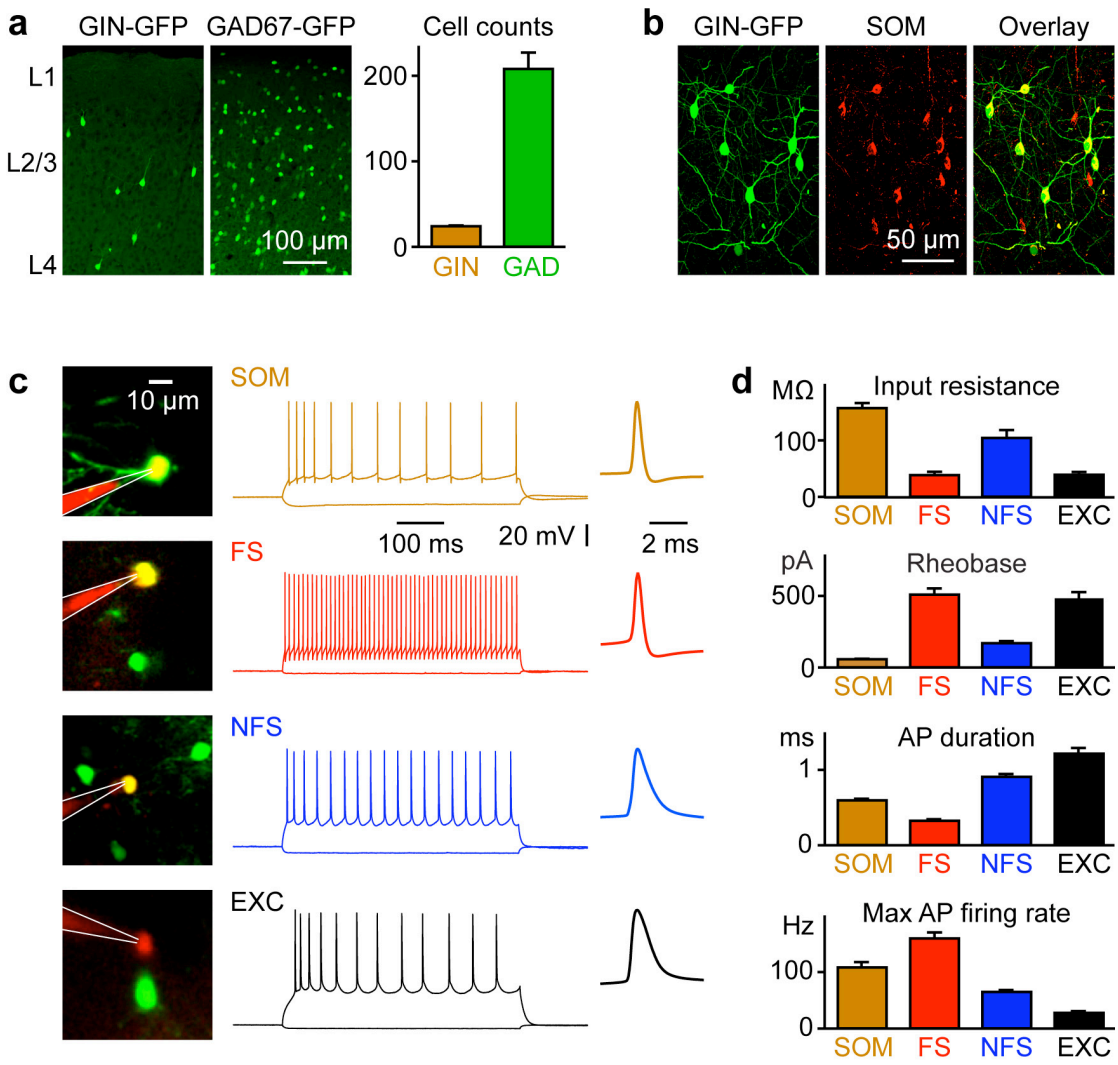

Supplementary Figure 1. Somatostatin-expressing GABAergic neurons form a sparse population of highly excitable cells. a, Confocal image stacks of 100 µm-thick fixed sections from layer 2/3 barrel cortex of GIN-GFP and GAD67-GFP mice (*left*). In layer 2/3 of the C2 barrel column we estimate that there are 24 ± 1 GIN-GFP neurons (n=3 mice) and 208 ± 19 GAD67-GFP neurons (n=3 mice) (*right*). Nearly all GABAergic neurons are labeled in GAD67-GFP mice, whereas only a small subset is labeled in GIN-GFP mice. **b**, A cluster of GIN-GFP neurons immunostained for GFP and somatostatin. Quantified in layer 2/3 barrel cortex across 5 mice, 100% (130 / 130) of GIN-GFP cells expressed somatostatin. GIN-GFP neurons are therefore termed SOM neurons in this study. However, it should be noted that GIN-GFP neurons represent a subset of somatostatin neurons, with only 44% (130 / 298) of somatostatin-expressing layer 2/3 cells being GFP-labeled. **c**, Whole-cell recordings of different classes of layer 2/3 neurons in awake head-restrained mice. Two-photon images (*left*) of GFP-labeled GABAergic neurons (green) together with the recording electrode filled with Alexa 594 (red), which for the recordings of GABAergic neurons colocalized with GFP fluorescence

Nature Neuroscience: doi:10.1038/nn.3051

(yellow). Current injections were used to assess intrinsic electrophysiological properties (*right traces*). **d**, The input resistance of SOM cells was higher than all other recorded cell types (SOM 157 ± 9 MΩ, n=49; FS 39 ± 6 MΩ, n=10; NFS 104 ± 14 MΩ, n=19; EXC 39 ± 5 MΩ, n=25). The rheobase of SOM cells was lower than all other recorded cell types (SOM 58 ± 3 pA, n=45; FS 510 ± 43 pA, n=10; NFS 170 ± 14 pA, n=19; EXC 484 ± 43 pA, n=25). Action potential duration of SOM cells was intermediate between FS and NFS GABAergic neurons (SOM 0.60 ± 0.02 ms, n=39; FS 0.32 ± 0.02 ms, n=9; NFS 0.91 ± 0.04 ms, n=17; EXC 1.22 ± 0.07 ms, n=22). Maximal firing rate of SOM cells was intermediate between FS and NFS GABAergic neurons (SOM 109 ± 9 Hz, n=15; FS 159 ± 11 Hz, n=10; NFS 65 ± 4 Hz, n=19; EXC 28 ± 3 Hz, n=18).

Nature Neuroscience: doi:10.1038/nn.3051

Supplementary Figure 2

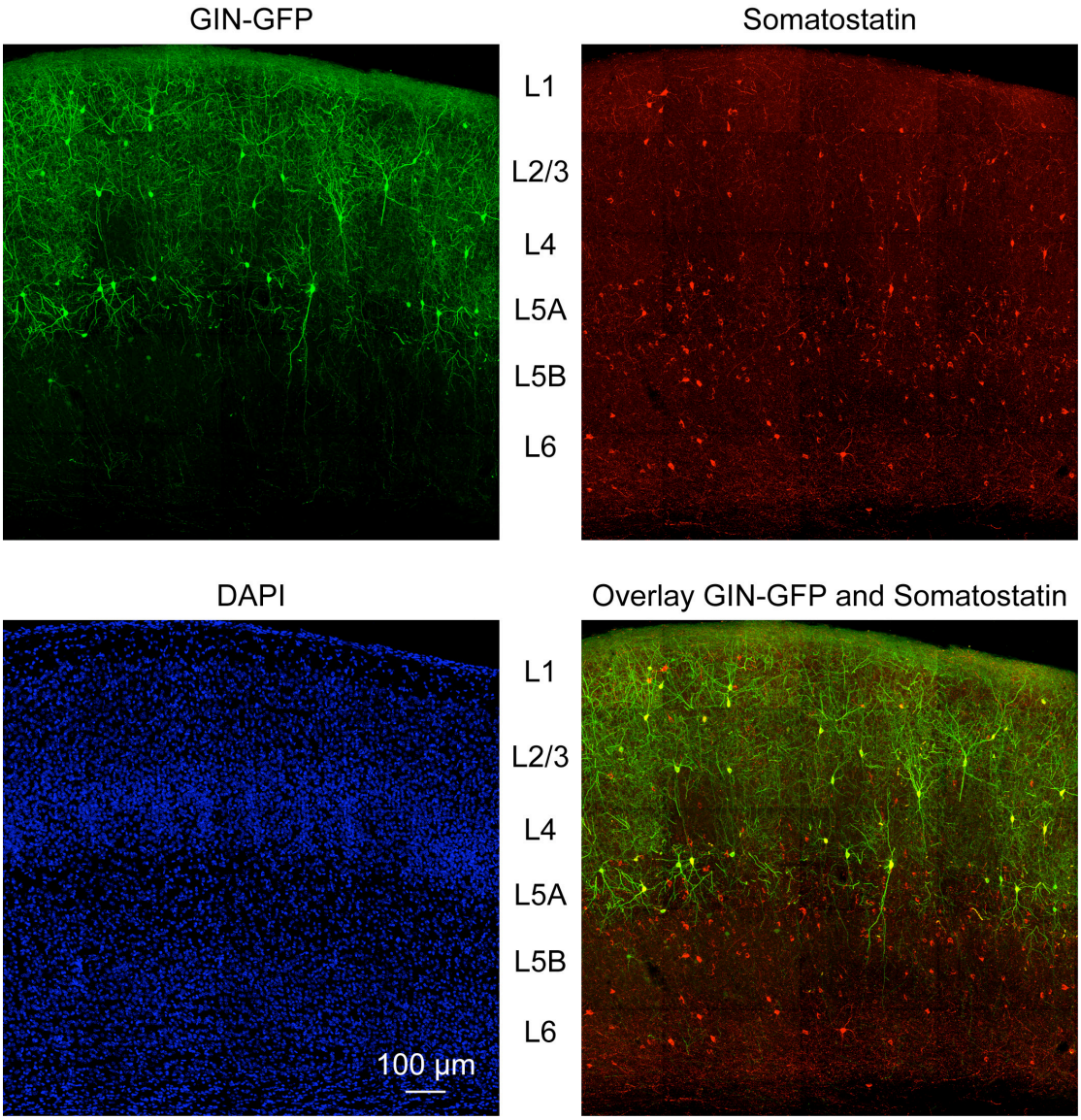

Supplementary Figure 2. GIN-GFP neurons are a subset of somatostatin expressing neocortical neurons. Each panel shows tiled images of the primary somatosensory barrel cortex of a coronal section obtained from a perfusion-fixed GIN-GFP mouse brain. The native GFP fluorescence was enhanced by immunostaining using an antibody against GFP (*upper left*, green). Immunostaining against somatostatin is shown in red (*upper right*). DAPI staining is shown in blue to visualize cortical layers and barrels (*lower left*). The overlay of GFP and somatostatin staining shows that all GIN-GFP labeled neurons express somatostatin, but that GIN-GFP neurons are a subset of all neocortical somatostatin expressing neurons. Note the nearly exclusive localization of GIN-GFP neurons in layers 2, 3 and 5A and their absence from layers 5B and 6.

Nature Neuroscience: doi:10.1038/nn.3051

Supplementary Figure 3

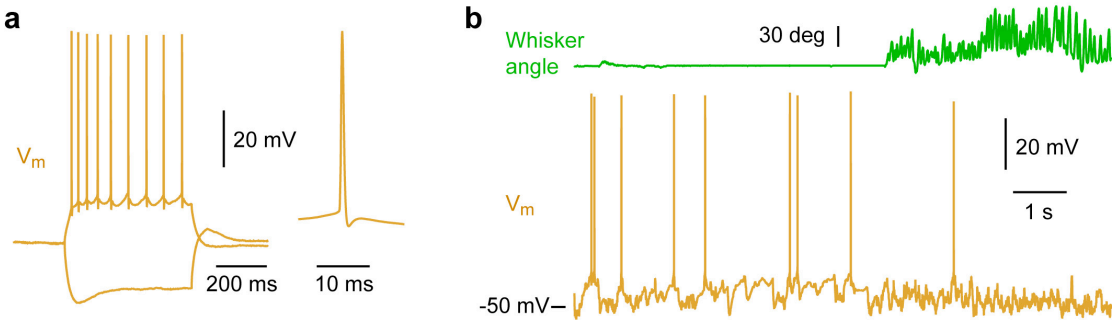

Supplementary Figure 3. Out of 30 recordings from GFP-labeled neurons in GAD67-GFP mice, we identified only one neuron with electrophysiological properties similar to the SOM neurons of GIN-GFP mice (this neuron was not included in further analyses). a, This SOM-like neuron recorded in a GAD67-GFP mouse had a firing pattern and action potential waveform typical of SOM neurons recorded in GIN-GFP mice. The action potential duration at half-maximal amplitude was 0.54 ms. The input resistance of this neuron was 199.8 MΩ. **b**, During quiet wakefulness this SOM-like neuron recorded in a GAD67-GFP mouse spontaneously fired action potentials at 1.7 Hz. During active whisking this SOM-like neuron hyperpolarized by 3.1 mV and reduced action potential firing rate to 0.4 Hz. Since immunohistochemistry shows that somatostatin-expressing neurons form a small subset of GFP-labeled neurons in GAD67-GFP mice (Tamamaki et al., 2000; Gentet et al., 2010), we consider it likely that this SOM-like neuron recorded in a GAD67-GFP mouse expressed somatostatin. Functionally identified, SOM neurons therefore appear to form a small fraction of GFP-labeled neurons in GAD67-GFP mice. Weak GFP fluorescence in SOM neurons of GAD67-GFP mice (Suzuki & Bekkers, 2010) likely reduced the probability of recording from SOM neurons in GAD67-GFP mice under our experimental conditions.

Nature Neuroscience: doi:10.1038/nn.3051

Supplementary Figure 4

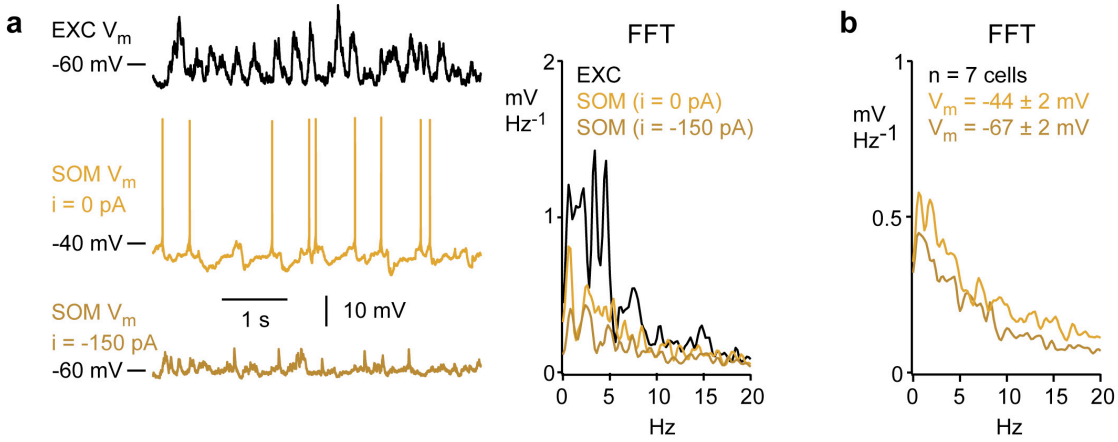

Supplementary Figure 4. Small-amplitude slow membrane potential fluctuations in SOM neurons. a, Whole-cell membrane potential recording from a layer 2/3 excitatory (EXC) neuron and a layer 2/3 SOM neuron during quiet wakefulness. The membrane potential of the excitatory neuron had obvious large-amplitude slow membrane potential fluctuations. Such slow membrane potential fluctuations were much less evident in the SOM neuron. Whereas the SOM neuron had a mean membrane potential around -45 mV, the excitatory neuron was much more hyperpolarized having a mean membrane potential of around -60 mV. One possibility is that the depolarized membrane potential of the SOM neuron might obscure slow membrane potential dynamics. We therefore hyperpolarized the SOM neuron by injecting -150 pA of current, which brought the mean membrane potential close to -60 mV (similar to that of the excitatory neuron). This hyperpolarization did not appear to enhance slow membrane potential fluctuations in the SOM neuron. Fast Fourier transform (FFT) analysis of the membrane potential quantitatively revealed that hyperpolarization of the SOM neuron did not enhance slow membrane potential fluctuations. **b**, Hyperpolarising current was injected in seven whole-cell recordings of SOM neurons. The FFT of membrane potential fluctuations from control and hyperpolarized periods were separately averaged across the seven recordings. There was no significant difference in the amplitude of slow membrane potential fluctuations comparing control with hyperpolarized periods (1-5 Hz fluctuations were non-significantly reduced by 18 ± 13 % during hyperpolarization, P = 0.16). Independent of the mean membrane potential, SOM neurons therefore have smaller-amplitude slow membrane potential fluctuations compared to excitatory neurons.

Nature Neuroscience: doi:10.1038/nn.3051

Supplementary Figure 5

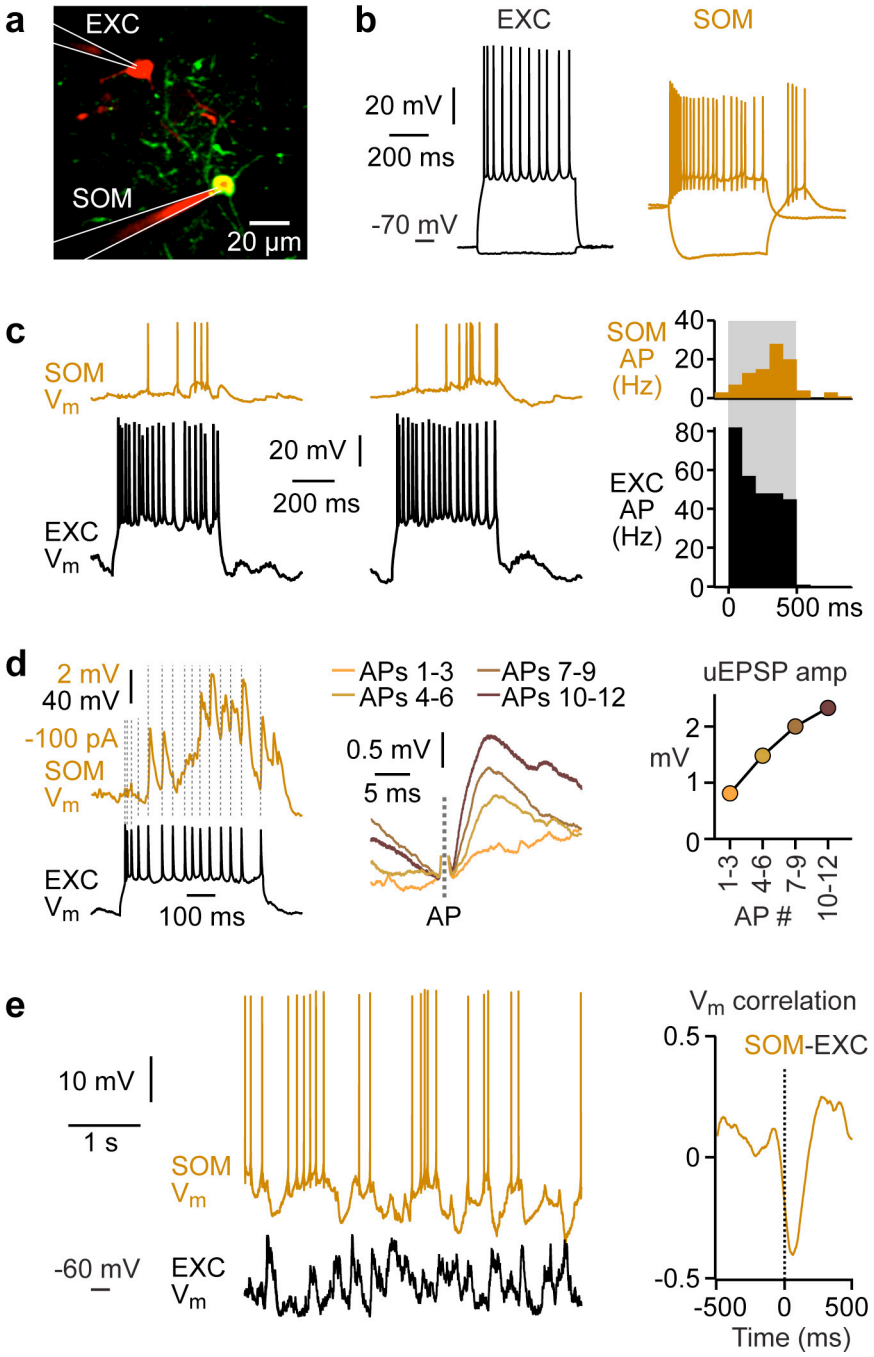

Supplementary Figure 5. The membrane potential fluctuations of a SOM cell were anticorrelated with a nearby excitatory neuron, despite a strong excitatory synaptic connection from the excitatory neuron onto the SOM cell. a, Two-photon image showing the presynaptic excitatory cell and the postsynaptic SOM neuron. **b**, The excitatory neuron and the SOM neuron responded with their respective characteristic firing patterns when depolarizing current was injected. Hyperpolarising current injections show that the SOM cell had high input resistance and it fired a rebound burst of spikes upon removal of the hyperpolarizing current. **c**, Simultaneous recording of membrane potential from the two neurons, revealed that action potentials

Nature Neuroscience: doi:10.1038/nn.3051

evoked in the excitatory neuron by current injection also drove postsynaptic action potentials in the SOM neuron. Action potential firing in the SOM neuron was delayed relative to those evoked by current injection in the excitatory neuron (*left* and *middle* show two example trials). The postsynaptic firing of the SOM neuron was robustly observed across trials. Averaging the spike rate across trials revealed that the action potentials of a single excitatory neuron drove the postsynaptic SOM cell to fire action potentials at a rate of ~20 Hz. **d**, To study the unitary EPSPs in the absence of postsynaptic firing, the SOM cell was hyperpolarized by injecting -100 pA of current. A single trial (*left*) shows that the first action potentials in the train (driven by depolarizing current injection into the excitatory neuron) did not evoke EPSPs in the SOM cell. The first detectable EPSP in this trial occured in response to the fifth action potential in the train. Later in the train, EPSPs were more reliably observed. Averaged across many trials, the EPSP recorded in the SOM cell were found to facilitate, with a small average EPSP observed in response to the first three action potentials (APs 1-3) in the train and larger responses being evoked by later action potentials in the train. This synaptic connection from an excitatory neuron to a SOM neuron recorded in an awake behaving mouse therefore shows prominent facilitating short-term synaptic dynamics, similar to those reported *in vitro* (Reyes et al., 1998; Silberberg et al., 2007; Kapfer et al., 2007; Fanselow et al., 2008). **e**, Spontaneous membrane potential fluctuations were anticorrelated in this synaptically connected pair of neurons. Although the excitatory neuron could monosynaptically depolarize the SOM neuron, the low firing rate of the excitatory neuron meant that it did not significantly contribute to the spontaneous membrane potential dynamics of the SOM neuron during our recording. The anticorrelated membrane potential dynamics of excitatory and SOM neurons observed in general were therefore also found even in a pair of neurons where the SOM neuron received monosynaptic input from the excitatory neuron.

Nature Neuroscience: doi:10.1038/nn.3051

Supplementary Figure 6

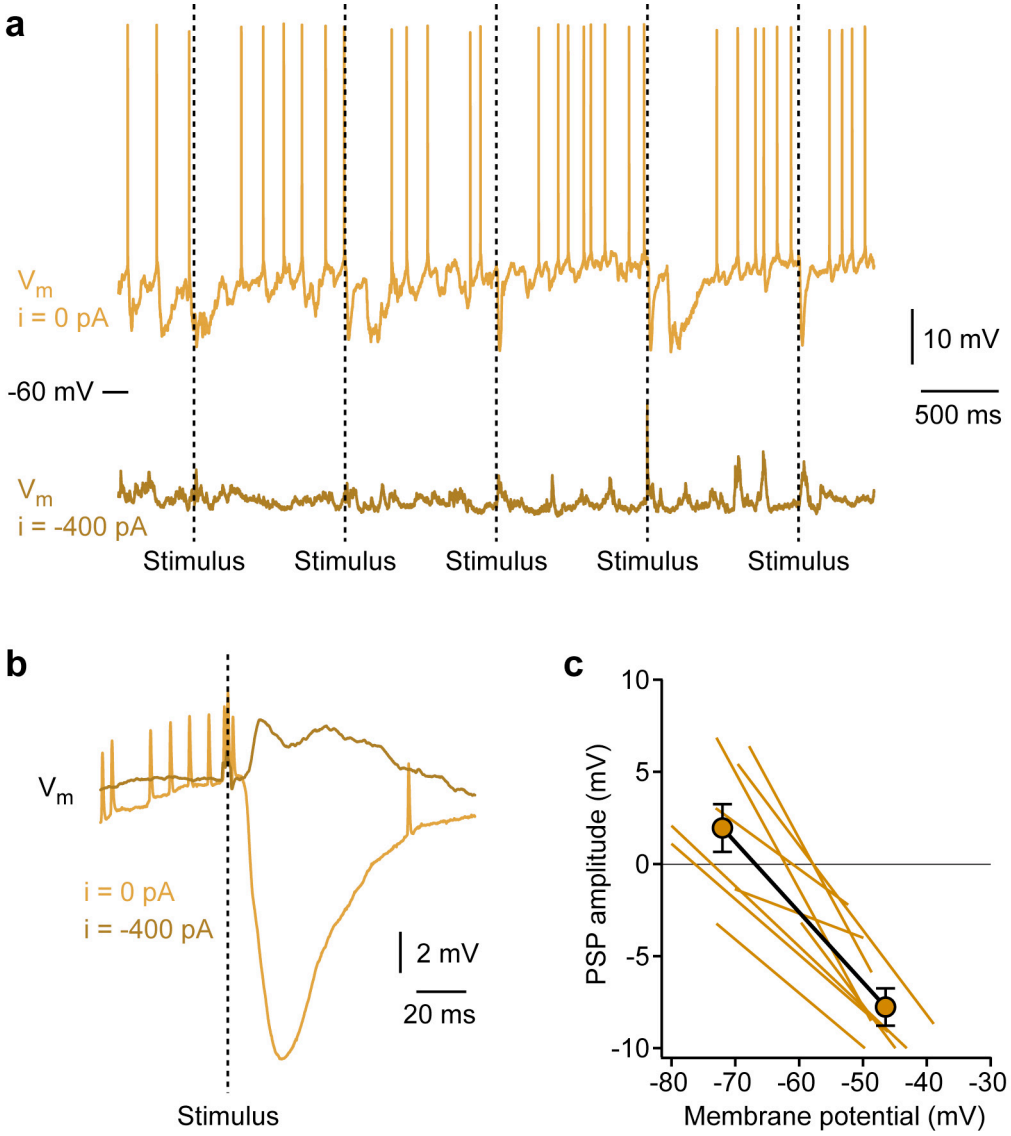

Supplementary Figure 6. Whisker deflection evoked a sensory response with a hyperpolarized reversal potential in SOM cells. a, Whole-cell membrane potential recording from a SOM neuron located in layer 2/3 of mouse barrel cortex. When no current was injected through the recording electrode (i=0 pA), brief single deflections of the C2 whisker evoked hyperpolarizing sensory responses. When the SOM neuron was hyperpolarized by injecting -400 pA of current, the same whisker deflections evoked depolarizing sensory responses. **b**, Averaged across all stimuli separately for control (i=0 pA) and hyperpolarized (i=-400 pA) conditions (same recording as shown in panel a). **c**, Each brown line indicates a recording from a SOM neuron in which the sensory response was recorded in control and hyperpolarized conditions. The reversal potential for the sensory response was estimated to be -68.9 ± 3.3 mV (n=9), suggesting that the sensory response in SOM neurons is dominated by synaptic activation of GABAergic conductances.

Nature Neuroscience: doi:10.1038/nn.3051

Supplementary Figure 7

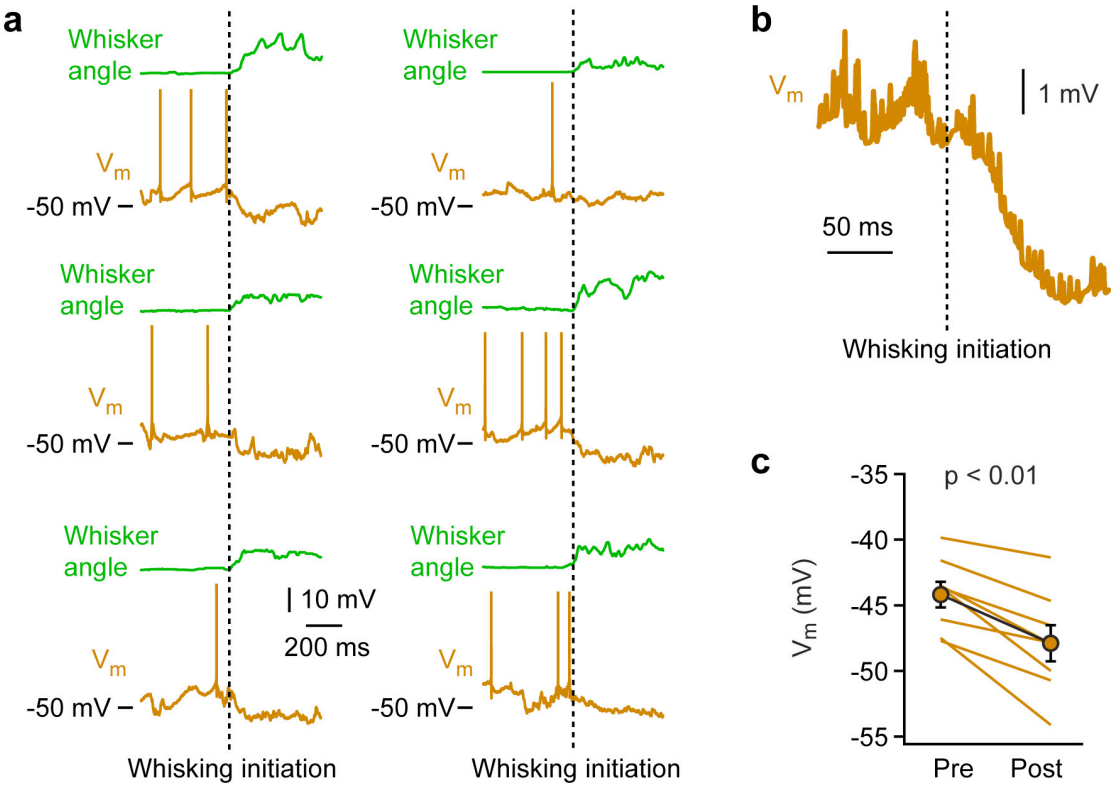

Supplementary Figure 7. SOM neurons hyperpolarized rapidly following initiation of active whisking. a, Example traces from the same whole-cell membrane potential recording of a SOM neuron during the onset of whisking. Membrane potential hyperpolarized after initiation of whisking. **b**, The membrane potential of SOM neurons averaged across all recordings and every whisking episode that had a clearly defined onset time. Membrane potential hyperpolarized shortly after initiation of whisking. **c**, Quantified for each of the 8 recordings which had at least 5 whisking episodes with a clearly defined onset time, membrane potential hyperpolarized in each SOM cell upon initiation of whisking ('Pre' denotes the 100 ms period before whisking onset; and 'Post' denotes the period 50-150 ms after whisking onset).

Nature Neuroscience: doi:10.1038/nn.3051

Supplementary Figure 8

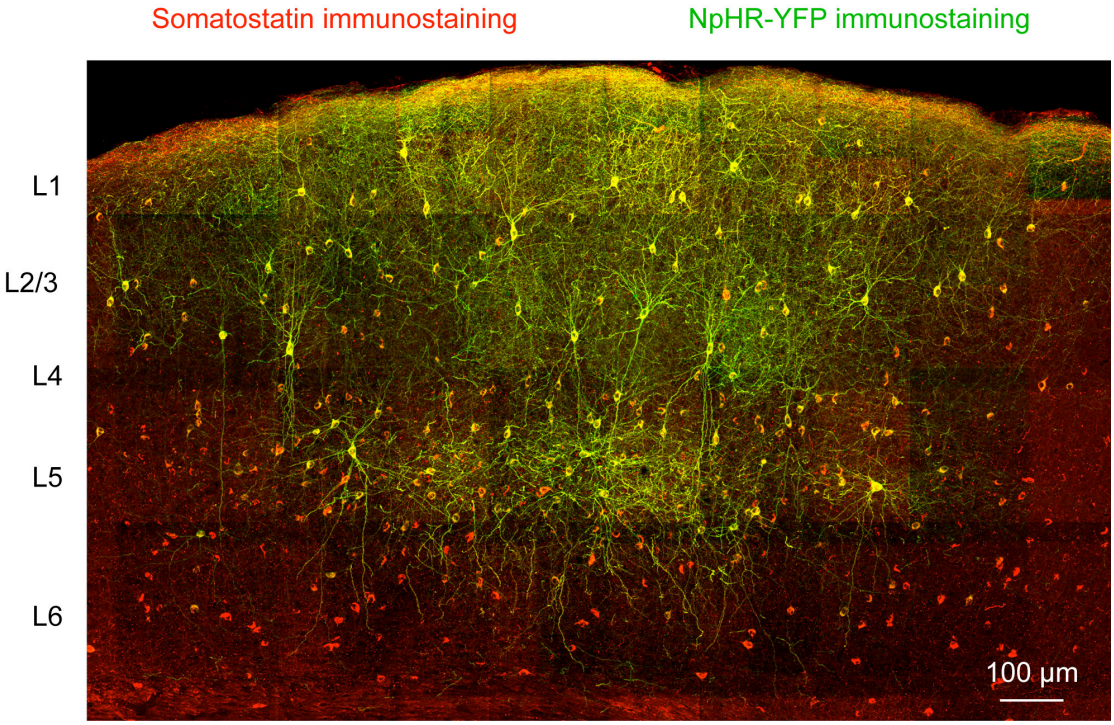

Supplementary Figure 8. Viral expression of NpHR3.0-YFP in SOM-Cre cells. NpHR3.0-YFP in a double-floxed inverted open reading frame adenoassociated viral vector was injected into the barrel cortex of SOM-Cre mice. After allowing several weeks for expression, the mouse was perfusion fixed with PFA and coronal sections were prepared. Somatostatin immunostaining is shown in red and GFP immunostaining for NpHR-YFP is shown in green with the overlap indicated by a yellow color. Neurons expressing NpHR-YFP were found in a ~1 mm diameter cortical area across layers 1 to 5. All neurons expressing NpHR-YFP also expressed somatostatin (182 NpHR-YFP expressing neurons across five slices).

Nature Neuroscience: doi:10.1038/nn.3051

Supplementary Figure 9

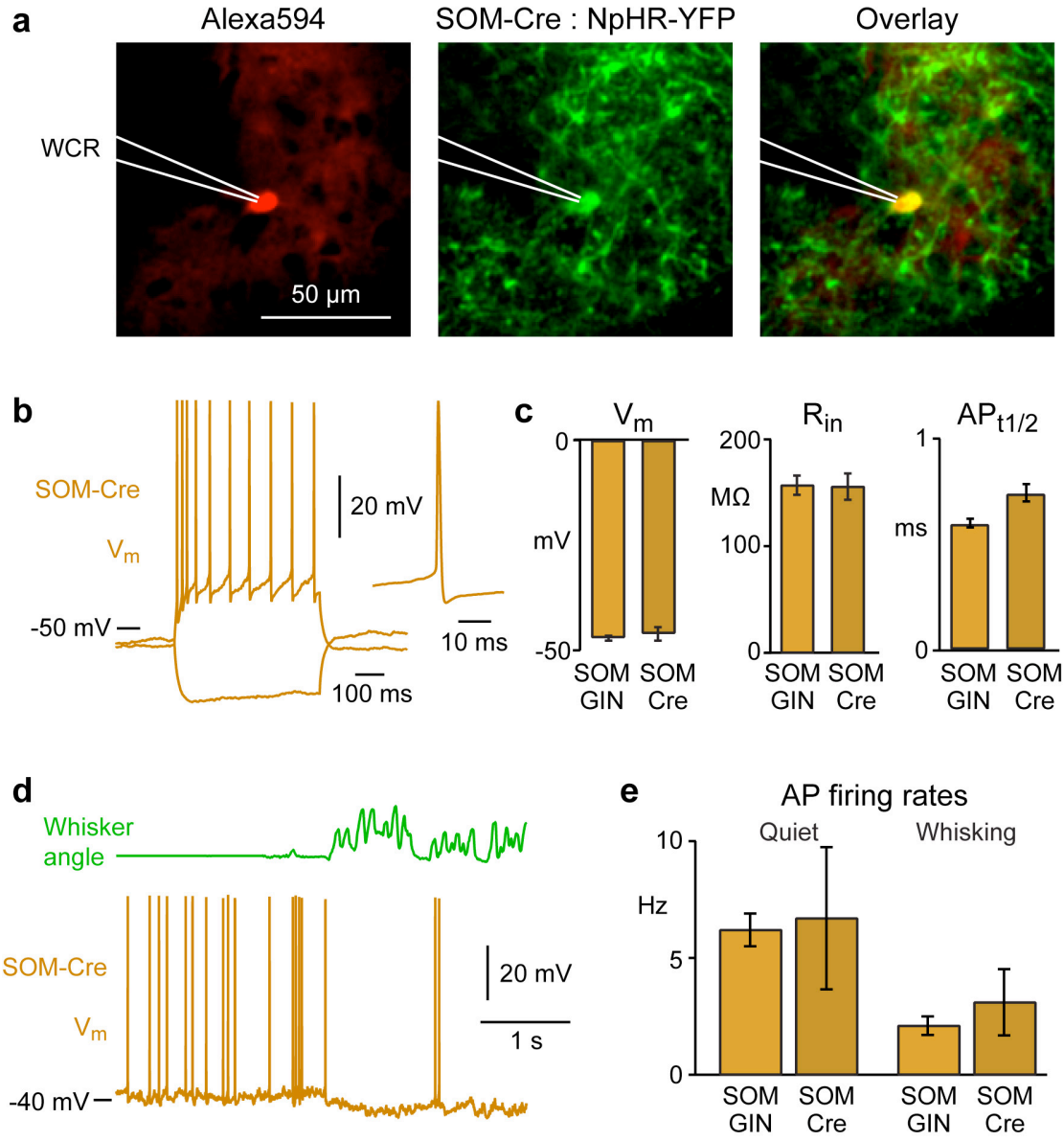

Supplementary Figure 9. SOM-Cre cells are similar to SOM cells recorded in GIN-GFP mice. a, Whole-cell recording (red fluorescence, Alexa594 in recording electrode) targeted to a SOM-Cre neuron (Taniguchi et al., 2011) expressing halorhodopsin fused to YFP (eNpHR3.0-YFP) delivered via a conditional AAV vector (AAV-DIO-NpHR) (Gradinaru et al., 2010). **b**, The firing pattern and action potential waveform of SOM-Cre neurons were similar to SOM neurons recorded in GIN-GFP mice. **c**, Across the population of recorded neurons, we found that the intrinsic electrophysiological properties of SOM-Cre neurons were similar to SOM neurons recorded in GIN-GFP mice. The mean membrane potential during quiet wakefulness of SOM-Cre neurons was similar to that of SOM-GIN cells (SOM-Cre -46.1 ± 1.6 mV, n=4; SOM-GIN -47.2 ± 0.6 mV, n=49). The input resistance SOM-Cre neurons was similar to that of SOM-GIN cells (SOM-Cre 156 ± 12 MΩ, n=4; SOM-GIN 157 ± 9 MΩ, n=49). The action potential duration at half-maximal amplitude in

Nature Neuroscience: doi:10.1038/nn.3051

SOM-Cre neurons was also similar to that of SOM-GIN cells (SOM-Cre 0.74 ± 0.04 ms, n=4; SOM-GIN 0.60 ± 0.02 ms, n=39). **d**, Whole cell recording of a SOM-Cre neuron during quiet wakefulness and active whisking without object contact. **e**, Action potential firing rates and their behavioral modulation were similar in SOM-Cre and SOM-GIN cells. During quiet periods SOM-Cre and SOM-GIN cells fired at higher rates (SOM-Cre 6.7 ± 3.0 Hz, n=3; SOM-GIN 6.2 ± 0.7 Hz, n=32) compared to during active whisking periods (SOM-Cre 3.1 ± 1.4 Hz, n=3; SOM-GIN 2.1 ± 0.4 Hz, n=32). We therefore conclude that SOM-Cre neurons have similar properties in general to SOM neurons recorded in GIN-GFP mice.

Nature Neuroscience: doi:10.1038/nn.3051

Supplementary Movie 1

GCaMP3 was expressed in excitatory neurons of the barrel cortex of an Emx1-Cre mouse using an AAV-FLEX vector. Fluorescence of layer 1 dendrites in the awake head-restrained mouse was imaged using a two-photon microscope. Whisker movements were filmed simultaneously with the calcium imaging. When the mouse moves its whiskers, the dendrites in layer 1 increase fluorescence.

Nature Neuroscience: doi:10.1038/nn.3051